LABORATORY WORK

Single-crystal gamma scintillation spectrometer

§1 Introduction. Brief overview of inorganic scintillators

Scintillation detectors currently have a wide range of applications for solving both tasks in nuclear physics experimental research, and production problems associated with the use of various types of ionizing radiation. Scintillation γ-detectors based on inorganic scintillators solve a wide range of tasks on the study of nuclear decay schemes in the framework of scientific programmes on γ-ray spectroscopy on accelerator beams (Gamma-Ball, scintillation anti-Compton shield HPGe, etc.), measurement of distribution of the input angular momentum populated in the various channels of reaction with heavy ions by measuring the multiplicity of γ-photon cascade (spin-spectrometers), measurement of probabilities of γ-transitions, analysis of the isotopic composition of radioactive compounds, determination of γ-radiation spectra passing through the shielding materials, determination of the absolute activity of sources, etc.

Table 1

Main characteristics of inorganic scintillators

Материал	Световыход, %	Темп.коэфф., %/°C	Постоянная времени спада, нс	Разрешение на 662 кэВ, %
NaJ(Tl)	100	- 0,3	250	6-8
CsJ(Tl)	45	0,01	1000	7-8,5
CsJ(Na)	85	-0,05	630	7-8,5
CsJ	4-6	- 0,3	16	30-32
$CdWO_4$	30-50	-0,1	14000	
$YAlO_3(Ce)$	40	-0,1	27	
$Y_3Al_5O_{22}(Ce)$	15	-	70	
BGO	20	- 1,2	300	9,5-12
LYSO	75	0,04	41	7-11
BaF_2	3	0	0,6 – 0,8	
$LaBr_3(Ce)$	130	0	26	2,5-3,5
$LaCl_3(Ce)$	70-90	0,7	28	2,5-3,5

It has become possible primarily due to the advantages of inorganic scintillators, such as high γ-radiation detection efficiency, fast operation speed, proportionality of the output signal amplitude to the value of the investigated radiation energy absorbed in the scintillator (see Table 1). The disadvantages of scintillation γ-spectrometer include low energy resolution compared with semiconductor γ-spectrometers. The energy resolution of scintillation γ-detectors based on common inorganic scintillators, such as $LaBr_3$, NaI(Tl), CsI(Tl), BaF_2, BGO has considerable

variation and ranges from 2% up to 32% (for γ-ray energy Eγ 662 keV).

$CdWO_4$ detectors have the highest density of inorganic scintillators, therefore, in case of necessity of manufacturing γ-detectors with small geometric dimensions special attention should be paid to this material, as well as to $Be_4G_3O_{12}$ (BGO) scintillators. BGO crystals have a higher absorption capacity compared with NaI(Tl), which allows reducing detector volume significantly.

Substantial drawbacks of BGO scintillators are low light yield, significant temperature dependence of the light yield, and, as a result, poor energy resolution and a temperature shift of the energy spectrum. In addition, it is worth noting that BGO has a minimal afterglow.

Another promising scintillator material is LYSO (Lu1, 8Y0, 2SiO5:Ce). This scintillator has characteristics similar to those of BGO in the energy resolution (from 7% to 11% for the γ-ray energy Eγ 662 keV). The density and effective atomic number values of LYSO are also close to the parameters of BGO. Therefore, LYSO scintillators have a greater value of detection efficiency than that of BGO. A distinctive feature of LYSO compared with NaI(Tl) and BGO is a considerably smaller temperature dependence of the light yield. This fact is determinant (in comparison with NaI(Tl) and BGO) when selecting γ-detectors intended for operation in various environmental conditions.

Next crucial advantage of LYSO scintillators in comparison with NaI(Tl) and BGO is a significantly smaller value of the scintillation decay time constant t - 40 ns compared with t ~ 250 and 300 ns for NaI(Tl) and BGO, respectively. This fact allows using LYSO scintillators at higher γ-radiation intensities, as it allows generating shorter pulses of the amplifiers of spectroscopic electronic spectrometer channels. Using LYSO scintillators in low-background measurements is limited by a high value of radioactivity resulting from the presence of Lu-176 isotope in the scintillator material.

In 2001, Saint-Gobain patented a new scintillator based on crystals – cerium-doped lanthanum halides. $LaBr_3$(Ce) and $LaCl_3$(Ce) scintillators have a higher energy resolution, short decay time ($LaBr_3$(Ce) ΔE(FWHM) ~3.2% for Eγ =662 keV), higher detection efficiency than that of NaI(Tl) and lower temperature dependence.

However, a serious drawback of single-scintillator γ-spectrometers is a complex shape of the energy spectrum. This fact complicates the processing of the measured spectra, especially in case when the monitored γ-source emits a cascade of γ-photons.

§2 Shape of the energy spectrum at detection of monoenergetic γ-photons with a single-crystal scintillation detector

Crystal scintillation is caused by secondary electrons in the interaction of γ-photons with matter (photoelectric effect, Compton effect and pair production). When the γ-energy is less than 1 MeV, the electron spectrum is determined by the photoelectric effect and the Compton effect.

In case of the **photoelectric effect,** γ-photon photoabsorption by one of atom electrons occurs, and therefore, an ionized atom and a free monoenergetic electron with kinetic energy equal to the energy of the absorbed γ-photons minus the electron-binding energy in the atom are formed in the scintillator material.

It is known that the photoelectric effect most likely occurs on the electron filling the *K*-

shell of the atom, the binding energy of the *K*-shell for iodine atoms is E_k=28 keV. Subsequently, the ionized atom transits into the ground state emitting a characteristic X-ray photon, which is normally absorbed in the scintillator material. In this case, all γ-energy remains in the scintillator. Figure 1 shows the spectrum of photoelectrons "1" and Compton electrons "2" in a thin scintillator (for a single Compton scattering of γ-photons), as well as the instrumental spectrum of the recorded γ-radiation.

The **Compton effect**, incoherent γ-photon scattering on free electrons, was discovered by an American physicist Arthur Compton in 1923 during his experiments with X-rays.

In case of **Compton effect** a scattered γ-photon has an energy $E_\gamma^{'}$ that depends on the scattering angle θ:

$$E_\gamma^{'} = \frac{E_\gamma}{1+\frac{E_\gamma}{m_0c^2}(1-\cos\theta)} \tag{1}$$

Depending on the γ-photon scattering angle θ, Compton recoil electron has the energy:

$$E_e = E_\gamma - E_\gamma^{'} = \frac{E_\gamma^2(1-\cos\theta)}{m_0c^2 + E_\gamma(1-\cos\theta)} \tag{2}$$

Kinetic energy of the recoil electron has a wide distribution restricted by the limits:

$$0 \le E_e \le \frac{E_\gamma}{1+\frac{m_0c^2}{2E_\gamma}} \tag{3}$$

Thus, the electron energy distribution of the Compton and photoelectric effect will always have a gap Δ*E*, see Fig.1, the value of which is determined by $E_\gamma^{'}$-energy of γ-photon scattered on angle θ = 180:

$$E_\gamma^{'} = \frac{E_\gamma}{1+\frac{2E_\gamma}{m_0c^2}}. \tag{4}$$

Value Δ*E* will decrease with increasing energy of γ-photons.

The energy distribution curve of the Compton effect electrons, see Fig.1, is determined by:

$$\frac{d\sigma_k}{dE_e} = \frac{\pi r_0 Z m_0 c^2}{E_\gamma^2}\left\{2 + \frac{m_0^2c^4E_e^2}{E_\gamma^2(E_\gamma - E_e)^2} + \frac{(E_e - 2m_0c^2)E_e}{E_\gamma(E_\gamma - E_e)}\right\} \tag{5}$$

and is characterized by a sharp increase in the region of maximum electron energy. For small-size scintillators the probability of multiple Compton scattering of γ-photons is low, and therefore, the continuous spectrum of recoil electrons detected in the scintillator will be determined by the process of single scattering. The spectra of Compton "2" and photoelectrons "1" for this case are shown in Fig.1. The ratio of the areas under distributions "1" and "2" is

determined by the ratio of the cross-sections of the Compton effect to the photoelectric effect for the scintillator material, respectively.

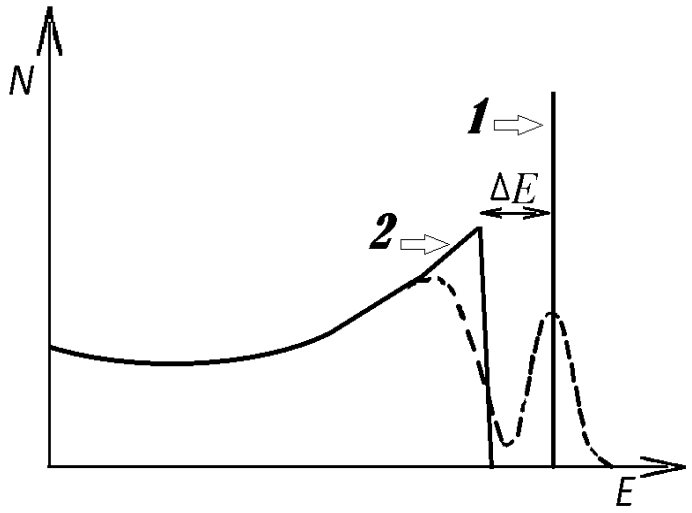

Fig.1. *Energy spectrum of photoelectrons "1" and Compton electrons "2" in a thin scintillator (for a single γ-photon scattering).*

Value ΔE determines the energy gap of the distributions above.

Dashed curve indicates the instrumental energy spectrum of the recorded γ-radiation.

Scintillator and photoelectric processes in the scintillation photodetector are purely statistical phenomena. Therefore, at the detector output monoenergetic electrons provide pulse amplitude distribution V described by the normal law:

$$\frac{dn(V)}{dV} = \frac{1}{\sigma\sqrt{2\pi}} e^{-\frac{V-V_0}{2\sigma^2}} \tag{6}$$

where V_0 - average pulse amplitude, σ^2 - variance of normal distribution associated with the spectrometer energy resolution $R(E_e)$ as follows:

$$D(E_e) = \sigma^2(E_e) = \frac{R(E_e)E_e}{2\sqrt{2\ln 2}} \approx 0.42R(E_e)E_e \tag{7}$$

Value σ is defines the full width of pulse amplitude distribution at half maximum (FWHM) ΔV as:

$$\Delta V = 2{,}36 \times \sigma \tag{8}$$

As a result, the amplitude spectrum of the scintillation detector will have a shape indicated in Fig.1 by a dashed curve. Peak "1" shown in Fig.1 is formed at the photoelectric absorption of γ-photons, and is called "**photopeak**".

As the size of the scintillator increases, the probability of multiple Compton scattering of γ-photons grows, which leads to a redistribution of pulses in the continuous spectrum "2" into a high-energy one. Moreover, there is a redistribution of events from distribution "2" into the

distribution forming the "**total absorption peak**" coinciding with the **photopeak** of distribution "1." This is due to the fact that after multiple Compton scattering a part of γ-photons loses a significant amount of energy and undergoes photoelectric absorption. The total kinetic energy of the electrons resulting from all the processes occurring in the scintillator will be the same as in case of a single photoelectric effect.

When the photon energy is several MeV, it is this process that in large-size crystals makes the main contribution to the formation of the total absorption peak.

At the energy condition $E\gamma > 2m_0c^2$ ($E\gamma > 1.02$ MeV) started a new process of interaction.

There're electron-positron pair production processes in which γ-photon energy is spent on the creation of an electron and a positron, as well as on the transfer of kinetic energy to them:

$$E_\gamma = 2m_0c^2 + E_{e^-} + E_{e^+} \quad (9)$$

In the formation of electron-positron pairs inside the scintillator, particles lose energy to a full stop, and after moderation a positron annihilates with one of the atomic electrons forming two annihilation γ-photons with $E\gamma$ = 511 keV. If both γ-photons are absorbed in the scintillator, the pulse entering the total absorption peak is formed. If one or both γ-photons leave scintillator without interaction, the spectrum will demonstrate peaks of "single escape" and "double escape" with energies $E_{SE} = E\gamma - 0.511$ MeV and $E_{DE} = E\gamma - 1.022$ MeV, respectively.

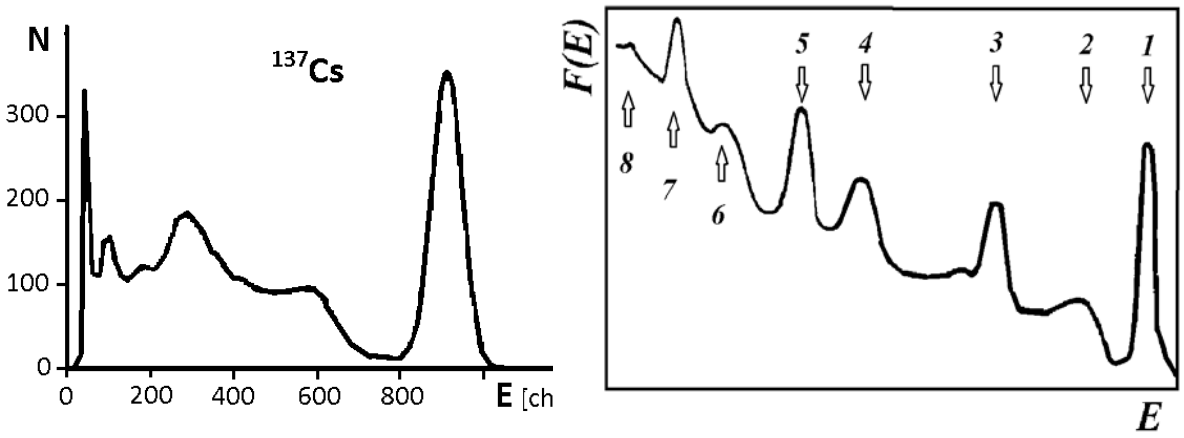

Fig. 2. (On the left) The energy spectrum of γ-source ^{137}Cs, $E\gamma$ = 662 keV, obtained by means of a NaI(Tl) scintillator.
(On the right) Typical energy spectrum F (E) when registering γ-photons with energy Eγ> 1.02 MeV.
Figures indicate characteristic peaks:

1. *total absorption peak;*
2. *upper limit of the Compton distribution;*
3. *single escape peak;*
4. *double escape peak;*
5. *annihilation radiation peak;*
6. *radiation leakage peak;*
7. *characteristic radiation peak;*
8. *bremsstrahlung.*

Detailed explanations are given in the text

If one or both annihilation γ-photons interact in the scintillator, the region of Compton

distribution in the spectrum is populated

from

$E_{MIN} = E\gamma - m_0c^2$ до $E_{MAX} = E\gamma - 2m_0c^2/3$.

Due to the effect of leakage of electrons from the crystal the lower boundary E_{MIN} of this distribution will be blurred. For the NaI(Tl) and CsI(Tl) scintillators the influence of the effect of the pair production becomes obvious when registering high-energy γ-photons starting from energy $E\gamma$ ~ 2 MeV. With increasing energy E_γ, the height of the single- and double-escape peak increases, and at $E\gamma$> 5 MeV becomes greater than that of the total absorption peak.

At $E\gamma$> 8 MeV the total absorption peaks, as well as single and double escape peaks almost merge into a single broad peak.

In addition to the characteristic features of the spectrum existing due to the properties of γ-photons interaction with the scintillator matter there are several features of the shape of the spectrum associated with the geometry of the experiment, the scintillator environment material, in particular with the location of the shielding and collimators. This is due to the fact that γ-photons produce secondary radiation in the materials surrounding the detector, which can interact with the scintillator not only contributing to a continuous distribution of the spectrum, but also causing formation of new spurious peaks in the spectrum. A striking example of a spurious peak is an "annihilation radiation peak", $E\gamma$ = 511 keV, occuring as a result of detection of a single annihilation γ-photon in the process of pair production exteriorly to the scintillator material.

Compton scattering is also the main cause of the radiation coming from the scintillator shielding and thus it is the hardest to eliminate, as it is formed at any values of energy Eγ.

The energy of the scattered photons is weakly dependent on angle θ at large scattering angles (see 1). Therefore, all the γ-photons reflected from the rear walls of the shielding and the elements surrounding the scintillator and detected in the scintillator will form the "**backscattering peak**". The backscattering peak position in the energy spectrum is given by:

$$E_{\gamma(\min)} = \frac{E_\gamma}{1 + 2E_\gamma / 2m_0c^2} \qquad (10)$$

Next to the backscattering peak in the low-energy region of the spectrum, there is another spurious peak. This is a "**characteristic radiation peak**", the main feature of which is the continuity $E = E_k$ of its location in the energy spectrum. The source of the peak is the elements of the shielding material surrounding the scintillator. The detector shielding, while performing its main function of retention of high-energy γ-photons sent to the scintillator, simultaneously emits characteristic X-rays produced as a result of the **photoelectric effect** in the process of γ-photon absorption. Typically, lead with Ek = 72 keV is selected as the shielding material for the detector, and the peak of the characteristic radiation corresponds to the energy $E\gamma$ = 72 keV. In order to reduce the contribution of this peak to the spectrum, multilayer screens made of a material with a decreasing atomic number Z are used. Conventionally, the surface of the lead house is first covered with a cadmium sheet with the thickness of H ~ 1 mm and with copper foil (H ~ 0.1 mm).

Thus, the shape of the energy spectrum of the scintillation γ-spectrometer is quite unique for each detector and depends on the geometry of the scintillator location relative to the shielding, collimator and the radiation source, as well as the materials of the above-mentioned

elements of the γ-spectrometer.

Under these conditions, in the γ-spectrum the total absorption peak will be least subject to distortion, because its shape is insignificantly influenced by the scattered γ-radiation. For this reason, the absolute or relative intensity of the γ-source can be conveniently determined by the ratio of the areas under the total absorption peaks of the corresponding γ-transitions. The ratio of the number of γ-photons $N_Ф$, that give all their energy in the crystal, to the total number of detected γ-photons $N_П$ is called the **photoelectric contribution** P(Eγ).

$$P(E\gamma)= N_Ф / N_П \qquad (11)$$

Experimentally the photoelectric contribution is determined as the ratio of the area under the total absorption peak to the area under the full spectrum.

The ratio of γ-photons completely absorbed in the crystal to the number of γ-photons N_0 caught in the crystal is called the **detection efficiency in the total absorption peak** or, which is not entirely correct, **photoefficiency** of the spectrometer.

$$\varepsilon_Ф(E\gamma)= N_{Ф\,/}\ N_0 \qquad (12)$$

The **total detection efficiency** of γ-photons is determined by the ratio of the total number of detected γ-photons $N_П$ to the number of γ-photons N_0 caught in the crystal:

$$\varepsilon(E\gamma)= N_{П\ /}\ N_0 \qquad (13)$$

The **detection efficiency in the total absorption peak** and the **total detection efficiency** are connected through the parameter of **photoelectric contribution** of the spectrometer:

$$\varepsilon_Ф(E\gamma) = P(E\gamma) \times \varepsilon(E\gamma) \qquad (14)$$

It should be noted that definitions (12) and (14) are strictly valid only in the case of detection of monoenergetic γ-photons, i.e. in one act of decay the source emits a γ-photon or a group (cascade) of γ-photons, provided that the time resolution of the scintillator and spectrometer equipment are capable of identifying these events of successive γ-emission as different. In the case of γ-sources “simultaneously” emitting several γ-photons (quite an ordinary case for on-line γ-spectroscopy on a heavy-ion beam) it is necessary to take into account their multiplicity Mγ. For example, for the events with Mγ=2 the area of the spectrum under the peak “γ1” is calculated by the product of prior defined values $\varepsilon_Ф(E\gamma1)$ of the probability of detecting the first γ-photon in the total absorption peak and (1- ε(Eγ2) of the probability of failing to detect the second γ-photon at all, as the energy emitted due to any interaction of the second γ-photon in the detector will be summed with the value Eγ1 and "take" the point of the event in the spectrum “out” of the total absorption peak Eγ1. Since this laboratory work does not consider cascade γ-transitions and sources with Mγ>2, detailed information can be found in [2].

From (14) one can conclude: the larger the crystal is and the better the γ-photon source is collimated, the higher the efficiency of the spectrometer is in the detection of the total absorption peak.

The lower limit of sensitivity of the spectrometer in the detection of the total absorption peak Eγ = 0.662 MeV by a scintillation detector with a NaI(Tl) sensitive volume V ~ 500 cm^3 is I ~ 10^{-14} Ci/g, which allows one to measure the spectra of γ-sources with the activity lower than natural. This limit is conditioned by its own background of crystal materials, shielding and structural elements, where the major contribution is made by K^{40}.

§3 Photomultiplier tubes

Photomultiplier tubes (PMTs) are the most common photodetecting converters of scintillation burst photons into electric pulses. The general view of the photomultiplier tube is shown in Fig. 3. The key parts of the PMT are photocathode, focusing electrode, dynode system of electrodes and anode. All parts of the PMT are arranged in a high vacuum in a glass (typically) container, the front part of which serves both as a window and a photocathode, and the rear part ensures a vacuum-tight electric contacts of the PMT dynode system with the voltage divider.

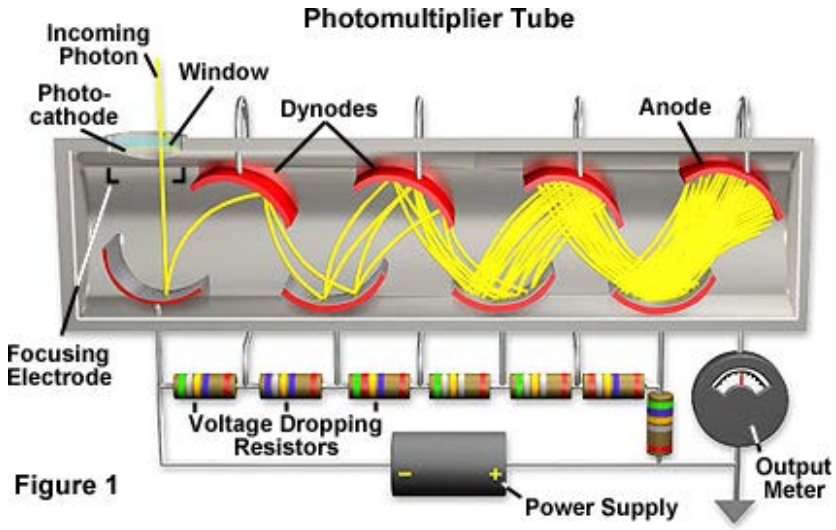

Fig. 3 Schematic view of the photomultiplier tube.
The figure is taken from the web site
http://learn.hamamatsu.com/articles/photomultipliers.html

The photocathode is a translucent multialkaline layer on the inner surface of the window. The photocathode material is alkali metals, as the electron output work A_e is significantly less than the energy of scintillation photons. (Cesium A_e = 2.1 eV, Potassium A_e = 2.1 eV) The window material is quartz, uviol, borosilicate or ordinary glass depending on the desired range of wavelengths of photon transmission. A window can have an inner concave surface to reduce the spread of path lengths (and thus the uncertainty of anode pulse rise time) of the electrons up to the first dynode. For this purpose there is also a focusing electrode system, which is especially important for the temporal characteristics of the PMT.

As a result of photon interaction with photocathode material it emits electrons that are picked up, accelerated by an electrostatic field and focused on the first dynode of the multiplier system. Accelerating and focusing field allows accelerating photoelectrons in the gap "photocathode-1st dynode" up to the energies of several hundred electron-volts, which allows one

to knock out several secondary electrons on the first dynode. The PMT divider is designed for creation of a potential difference in the electrodes of the dynode system providing optimum value of the secondary emission coefficient $\beta \sim 4 \div 5$. The electrons knocked out from the 1st dynode of the system are focused, accelerated and knock out electrons from the 2nd dynode, etc. At the end of the controlled process of multiplication in the PMT dynode system the electron flux having the same shape as the scintillation burst reaches the anode and produces a voltage drop on the input resistance of electronic equipment. It is noteworthy that the PMT as an electronic device is an electric current source and has very high output resistance, thus, the voltage amplitude of the anode pulse within a wide range is determined by the load resistance.

The structure of the anode circuit strongly depends on the connection of the high voltage to the PMT. There are two ways to connect the PMT (see. Fig.4): "grounded cathode" and "grounded anode", or "+ HV" and "-HV", respectively.

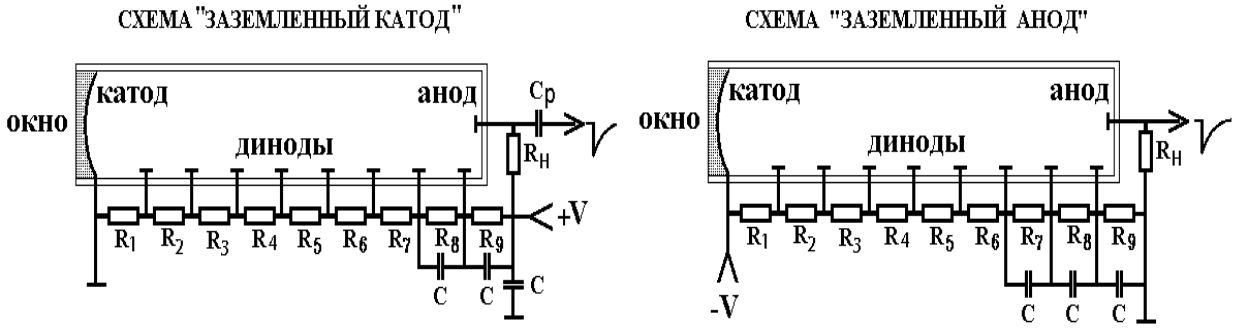

Fig. 4 Connection diagram of high-voltage divider of the 8-dynode PMT. On the left - the diagram "grounded cathode", on the right – the diagram "grounded anode." The system of resistors R_1 - R_9 forms a multi-step voltage divider that creates the appropriate potential differences between the PMT dynodes. Resistor R_H is the load resistor. Capacitances C stabilize the potentials on the last PMT dynodes at the moment when an avalanche of electrons passes through the PMT. Capacitance C_P is a coupling capacitance.

Each of the diagrams has both advantages and disadvantages. In the first case the PMT photocathode is at ground potential, therefore, the anode is at positive polarity voltage of several kilovolts, and the anode signal pickup is performed by the high-voltage capacitor of the coupling capacitance C_P.

In this laboratory work, the high-voltage power supply to the PMT corresponds to "-HV", when the PMT photocathode is at high-voltage potential of negative polarity, and thus, the anode is at ground potential, which simplifies the anode circuit significantly.

However, in this case the photocathode undergoes constant micro-discharges of leakage currents onto the PMT design elements and other elements at ground potential. This leads to a deterioration of the energy resolution. As noted above, the PMT is a current source, i.e. it has a very high output resistance, but in the anode circuit, even in the case of "-HV" divider, there is an R_H resistor (1KOm ÷ 20KOm) being a capacity leakage resistor and protecting the subsequent elements of the electronic circuit from destruction. For fast PMTs designed for fast scintillators, the choice of the resistance value R_H = 50 ohms is due to the need of agreement with the wave resistance of the coaxial cable.

§4 Block diagram of a scintillation spectrometer

Figure 5 presents a block diagram of a single-crystal scintillation spectrometer, which is used in this laboratory work.

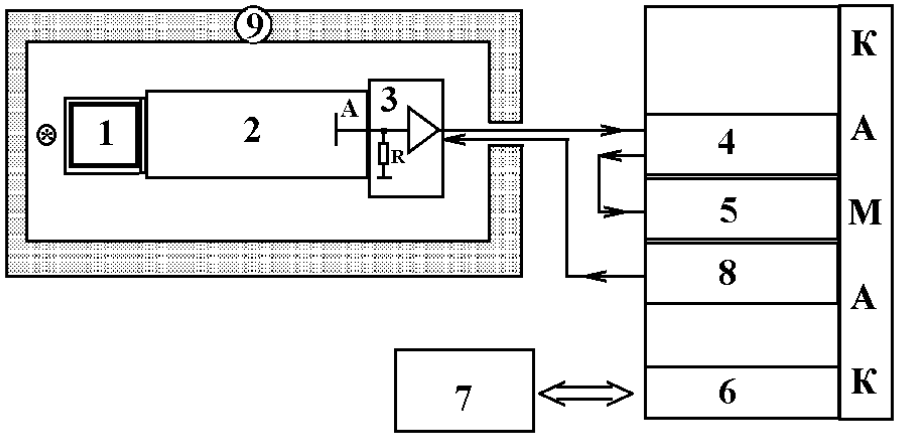

Fig. 5 *Block diagram of a scintillation spectrometer.*

The main elements of the scintillation spectrometer are:

1- *Scintillation crystal NaI(Tl) ∅63 ×63 mm;*
2- *Photomultiplier tube PMT-82 with a high-voltage resistive divider (the divider is not shown in the figure);*
3- *Emitter follower of the anode signal (optional);*
4- *Spectroscopic anode pulse shaping amplifier;*
5- *CAMAC ADC unit - 12-bit peak pulse converter "Amplitude-digit" PA24-K;*
6- *Crate controller CAMAC CC-009;*
7- *PC with interface controller CC-009 to collect and analyze information from the facility crate;*
8- *PMT high-voltage power unit;*
9- *Lead shielding of the scintillation detector.*

Scintillation crystal NaI(Tl) optically coupled to the PMT photocathode is placed in a light-tight sealed housing due to the high hygroscopicity of the scintillator. In order to increase light gathering from the scintillation burst the crystal is coated with a diffuse reflector (in our case - MgO).

As noted above, photomultiplier PMT-82 is used as a photodetector, it has a translucent antimony-cesium photocathode with a spectral response of a peak sensitivity at 350 ÷ 650 nm, which corresponds to the NaI(Tl) emission spectrum, the electrostatic electron focusing, and a 12-dynode louvre-type multiplying system.

The general view of the PMT-82 is shown in Fig. 6.

Fig. 6 *General view of the 12-dynode spectroscopic photomultiplier tube PMT-82.*

High voltage providing the required values of the potentials for each electrode of the PMT dynode system is supplied to the PMT divider from unit 8 - a high-stable voltage source (POLON 1904). High voltage is manually adjusted in the range of voltages V_{HV} = [1.0 V ÷ 2500 V]. Since in our case the PMT divider is connected according to the "grounded anode", the polarity of the V_{HV} is negative.

Anode pulse from the photomultiplier is fed through an emitter follower of anode signal 3 (optional) to shaping amplifier 4, where it is formed by manually-defined parameters of "integration time" and "gain" and is supplied to an ADC unit.

One of the tasks of the laboratory work is the study of the signal amplitude spectrum.
Thus, single-crystal scintillation γ-spectrometer can be characterized by the following parameters:
1) ***Energy resolution****;*
2) ***Luminosity*** *(determined as the ratio of the detected γ-photons to the number of the ones emitted by the source)*
3) ***Detection efficiency*** *(determined as the ratio of the detected γ-photons (area under the curve of the energy spectrum above a certain threshold E_{THRES}) to the number of γ-photons caught in the spectrometer.*
The efficiency depends on the energy of γ-photons and scintillator sizes.
4) ***Efficiency in the total absorption peak*** *(determined as the ratio of the γ-photons detected in the total absorption peak (area under the curve of the energy spectrum in the total absorption peak) to the number of γ-photons caught in the spectrometer.*

Fig. 7 *General view of a single-crystal γ-radiation scintillation spectrometer.*

§5 Instructions on how to perform laboratory work N2

This laboratory work is to be performed on a single-crystal NaI(Tl) γ-spectrometer, the block diagram of which is shown in Figure 5, as well as on single-crystal γ-detectors based on CsI(Tl) and BGO scintillators. CsI(Tl) and BGO scintillators with PMT-49 and PMT-82, respectively, are free of lead shielding and NaI(Tl) scintillator with PMT-82 is in the lead shielding to reduce γ-background. The upper lid of the shielding can be moved to gain access to the end surface of the scintillator. The accumulation of data is performed by a collection system based on CAMAC electronics and a PC providing both the accumulation of physical events in the data files, on-line analysis of events, and the subsequent off-line data analysis. A detailed description of the elements of the collection system, as well as the collection and analysis of experimental data programme are presented in Appendix 1.

In the process of work performance a number of γ-sources will be provided, both for graduation and calibration of γ-spectrometer, and for determination of the source by the characteristic γ-lines of total absorption peaks in the energy spectra. For this reason, the measurements should be carried out at constant values of the PMT high voltage, a fixed set of system parameters, in particular, the constant coefficients of spectroscopic pulse formation (gain factor, values of the voltage offset, the values of time integration and amplifier differentiation, etc.)

Task

1. Measure resistance R_H at the output of the PMT coaxial connector and determine the connection type for the PMT voltage divider. Switch on the CAMAC crate, computer and oscilloscope. Adjust the oscilloscope to the maximum sensitivity mode, "DC analysis", set the oscilloscope input resistance R IN = 1 Mohm and connect the cable from the PMT anode to the input of the oscilloscope. Increasing high voltage in increments of 100 V, observe the offset of the constant on the oscilloscope. No significant offset means that the PMT is light-tight. Determine the value of the PMT anode current offset at a load resistance by the rated values of the PMT dark current. Note that the value of the anode current will be slightly higher than the rated value due to the background scintillation pulses from NaI(Tl). Such a verification of the value of the PMT anode current is useful when operating photomultipliers without stationary housings, as it allows timely detecting the failure of the lightshield and avoiding the damage of the photodetector.

2. Measure the energy spectra of standard γ-sources at three values of HV (values to be obtained from the supervisor), process the spectra by determining the average values of the total absorption peak positions, their widths, areas under the peaks, etc. Plot the functions (linear and second-degree polynomial) of the energy calibration using the tecnique of least squares. Determine the range of application of the linear calibration. Measure the energy spectra of the γ-sources studied. Determine the energies of γ-transitions of the investigated sources by the positions of the total absorption peaks in the energy scale, which has been received in the energy calibration of the spectrometer. According to table of characteristic γ-transitions identify the investigated source.

3. Analyze the measured spectra and determine the parameters of the spectrometer:
   - detection efficiency;
   - detection efficiency in the total absorption peak;
   - spectrometer luminosity;
   - energy resolution.

4. Connect the PMT anode of NaI(Tl) detector to an oscilloscope and measure the anode pulse shape from this scintillator. Perform a similar procedure with scintillation detectors based on Cs(Tl) and BGO crystals. Conduct a comparative analysis of the shapes of scintillation signal from NaI(Tl), Cs(Tl) and BGO scintillators.

5. Prepare a report on the work done.